ARTICLE

Ro-vibrational Spectra of the Simplest Deuterated Criegee Intermediate CD$_2$OO†

Jun Li*

School of Chemistry and Chemical Engineering, Chongqing University, Chongqing 401331, China

Criegee intermediates are of significance in the atmospheric chemistry. In this work, the ro-vibrational spectra of the simplest deuterated Criegee intermediate, CD$_2$OO, were studied by a vibrational self-consistent field/virtual configuration interaction (VSCF/VCI) method based on a nine-dimensional accurate potential energy surface and dipole surface for its ground electronic state. The calculated fundamental vibrational frequencies and rotational constants are in excellent agreement with the available experimental results. These data are useful for further spectroscopic studies of CD$_2$OO. Especially, the rotational constants for excited vibrational levels are essential for experimental spectral assignments. However, the infrared intensities from different resources, including the current computation, the experiment, and previous calculations at the NEVPT2 and B3LYP levels, deviate significantly.

Key words: Criegee intermediates, Vibrational spectra, Rotational constants, Multimode calculations, Potential energy surface

I. INTRODUCTION

The Criegee intermediates (CIs, R$_1$R$_2$COO) have been postulated to be involved in the reactions between alkenes and ozone [1], which are common and significant in the atmospheric chemistry [2]. Due to the large exothermic nature of these reactions, the nascent CIs are often very hot with large amount of internal energy, and are thus highly reactive with short lifetimes. Therefore, their important roles in the atmosphere were only identified recently thanks to a breakthrough in generating such short-lived species in the laboratory [3]. Indeed, it has been established that CIs are very active in several important atmospheric reactions with rapid rates and are potentially important initiators for atmospheric oxidation [4–7].

The simplest CI is formaldehyde oxide, CH$_2$OO, whose geometries and vibrational spectrum have been studied extensively by microwave [8–10] and infrared [11–13] spectroscopic techniques. These spectra can provide valuable information for their identification and structural characterization of these metastable intermediates. Theoretical models are essential in assigning their spectroscopic features. Indeed, very accurate fundamental frequencies and intensities have been determined on a high-quality potential energy surface (PES) and dipole moment surface (DMS) for CH$_2$OO [14, 15],

compared to the observations [11]. Further, the large deviation between theory and experiment for the ν_5 mode (CH$_2$ rock), 18 cm^{-1}, urged experimentalists to improve the spectroscopic resolution and made reassignments [12]. Besides, the rotational constants, for both ground vibrational states and excited vibrational states, were well reproduced on the high-quality PES [10]. The excellent agreement with experiment validates the excellent performance of the PES.

To further understand the chemistry and physics of CH$_2$OO, its deuterated isotopologue, CD$_2$OO, has been investigated as well [8, 9, 16]. The four vibrational bands observed at 852, 1017, 1054, and 1318 cm^{-1} were assigned to the OO stretching (ν_6), two distinct in-plane OCD bending (*cis* ν_5 and *trans* ν_4), and the CO stretching mode (ν_3), respectively [16]. The theoretical positions of these bands computed at the NEVPT2/AVDZ and B3LYP/AVTZ levels were in fair agreement with experiment. However, the experiment-theory deviations in these infrared intensities were quite large [16]. In this work, we report theoretical simulations on the ro-vibrational spectra of CD$_2$OO using the accurate PES and DMS, which have been successfully used to reproduce spectra of CH$_2$OO very well [14].

II. CALCULATION DETAILS

A full-dimensional PES of CH$_2$OO [14] has been developed using the permutation invariant polynomial-neural network (PIP-NN) method [17, 18] based on ∼50,000 points computed at the level of CCSD(T)-F12a/AVTZ [19]. The DMS [14] was fit to point-charge

TABLE I Comparison of vibrational wavenumbers (in cm^{-1}) of CD$_2$OO and D-isotopic ratios from various methods.

Mode	CD$_2$OO			D-isotopic ratio		
	VCI-5(this work)	NEVPT [16]	Expt. [16]	VCI-5(this work)	NEVPT [16]	Expt. [16]
ν_1	2405.8	2450		0.7636	0.7780	
ν_2	2193.6	2235		0.7280	0.7376	
ν_4	1063.3(94)	1058(55)	1054(30)	0.7417	0.7257	0.7350
ν_3	1318.3(24)	1328(187)	1318(39)	1.0256	1.0200	1.0250
ν_5	1013.7(25)	1016(13)	1017(11)	0.8366	0.8328	0.8382
ν_6	863.1(70)	839(89)	852(37)	0.9309	0.9406	0.9370
ν_7	466.8	464		0.8883	0.8755	
ν_8	691.2	673		0.8043	0.7890	
ν_9	477.5	470		0.7683	0.7756	

expression using the PIP method [20] based on ~46,000 points calculated at the level of CCSD(T)-F12a/AVDZ. Using the PES and DMS, the MULTIMODE approach [21] was employed to calculate the ro-vibrational spectra of CD$_2$OO. Briefly, the mass-scaled normal mode coordinates were used in the Watson Hamiltonian [22] and the potential is expressed in a hierarchical n-mode representation. In this work, the potential is truncated with up to 6-mode terms. Firstly, the $J=0$ vibrational levels were determined using the vibrational self-consistent field (VSCF) approach [23, 24]. The vibrational wavefunction was further expanded in terms of the eigenfunctions of the VSCF Hamiltonian in order to account for coupling among the nine vibrational modes. This virtual configuration interaction (VCI) method [25, 26] typically improves the computational results, and was used here with up to 5-mode excitations. Tests show that the fundamental vibrational frequencies are converged within 2 cm^{-1}. The infrared intensities were determined according to the method given in Ref.[27]. For rotationally excited states ($J>0$), the VCI basis is a direct product of the VSCF basis and symmetric top wavefunctions $|J, K, 0\rangle$, and the Hamiltonian matrix is diagonalized to determine the ro-vibrational levels [26]. Only $J=0$ and $J=1$ VCI calculations are required to obtain the rotational constants of each specific vibrational state by using the relation [28] between the calculated ro-vibrational states and the rotational constants: $E(1_{01})=B+C$, $E(1_{11})=A+C$, $E(1_{10})=A+B$, with respect to each specific vibrational state $E(0_{00})=0$.

III. RESULTS AND DISCUSSION

In Table I, the $J=0$ CD$_2$OO anharmonic frequencies calculated by the VCI-5 method are compared to both experimental and previous theoretical values [16]. The agreement with the recent experimental data [16] is quite good. The calculated fundamental vibrational frequencies are 1063.3, 1318.3, 1013.7, and 863.1 cm^{-1} for ν_4, ν_3, ν_5, and ν_6, respectively. The cor-
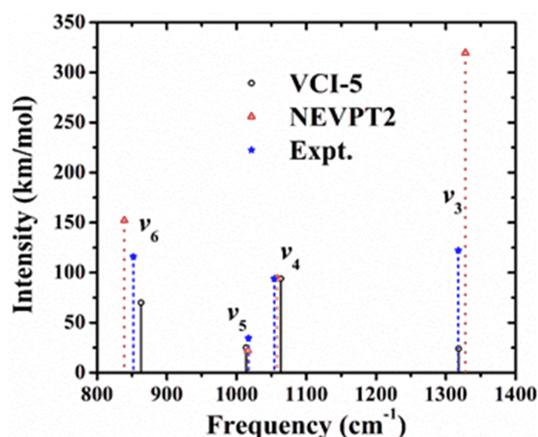

FIG. 1 Comparison of the infrared spectrum of CD$_2$OO obtained from experiment and theory (VCI-5 and NEVPT2). The experimental and NEVPT2 values are normalized with the intensity of the ν_4 line calculated by VCI-5.

responding experimental assignments are 1054, 1318, 1017, and 852 cm^{-1}, respectively [16]. The deviations are $+8.7$, $+0.3$, -3.3, and 11.1 cm^{-1}, respectively, comparable to those calculated at the NEVPT2 level $+4$, $+10$, -1, -13 cm^{-1} [16]. It is noted that for CH$_2$OO, the NEVPT2 calculated frequencies deviated significantly from the experiment [11], and VCI-5 results agreed very well with the experiment, thanks to the accurate full-dimensional PES and DMS, as well as the sophisticated VCI method [14]. In Table I, the deuterated-isotopic (D-isotopic) wavenumber ratios, defined as $v(CD_2OO)/v(CH_2OO)$, are compared. The experimental results are 0.7350, 1.0250, 0.8382, 0.9370, compared to 0.7417, 1.0256, 0.8366, 0.9309 by VCI-5, or 0.7257, 1.0200, 0.8328, 0.9406 by NEVPT2 [16].

FIG. 1 displays the VCI-5 calculated infrared spectrum for CD$_2$OO with the experimental and NEVPT2 [16] spectral positions and relative intensities for comparison. The intensities of the latter two were normalized according to the ν_4 intensity calculated by the VCI-

TABLE II Theoretical rotational constants of the ground and excited vibrational levels of CD$_2$OO, and shifts of them from the ground vibrational level.

Level	Description[b] [16]	Rotational constants/MHz			Shifts[a]/MHz		
		A	B	C	A	B	C
0_0	Ground	60269	11025	9289			
ν_1	a-CD$_2$ str.	59963	10986	9247	−306	−39	−42
ν_2	s-CD$_2$ str.	59840	11004	9259	−429	−21	−30
ν_3	CO str./CD$_2$ sci.	59978	11001	9259	−291	−24	−30
ν_4	OCD$_{trans}$ bend/OO str.	60207	10975	9240	−61	−49	−49
ν_5	OCD$_{cis}$ bend	60353	11031	9289	84	6	0
ν_6	OO str./OCD$_{trans}$ bend	60180	10984	9255	−88	−40	−34
ν_7	COO bend	60816	11017	9282	547	−7	−7
ν_8	CD$_2$ wag	60563	11031	9298	294	6	9
ν_9	Out-of-plane deform	60203	11046	9301	−66	21	12

[a] Given as the difference in rotational constant between the v=1 and v=0 levels.
[b] Vibrational mode specification.

TABLE III Comparison of ratios of rotational parameters in their ground and vibrationally excited states for vibrational modes of CD$_2$OO.

Mode	Sym.	B3LYP/aVTZ [16]			VCI-5 (this work)		
		A'/A''	B'/B''	C'/C''	A'/A''	B'/B''	C'/C''
ν_1	A'	0.9962	0.9978	0.9980	0.9949	0.9963	0.9953
ν_2	A'	0.9949	0.9988	0.9980	0.9929	0.9980	0.9966
ν_3	A'	0.9981	0.9962	0.9963	0.9952	0.9977	0.9966
ν_4	A'	1.0021	0.9997	1.0021	0.9990	0.9954	0.9945
ν_5	A'	1.0044	1.0024	0.9935	1.0014	1.0004	0.9998
ν_6	A'	1.0049	0.9959	0.9959	0.9985	0.9962	0.9961
ν_7	A'	0.9526	0.9949	0.9972	1.0091	0.9992	0.9990
ν_8	A''	0.9928	0.9973	1.0014	1.0048	1.0004	1.0008
ν_9	A''	1.0443	1.0038	1.0012	0.9989	1.0018	1.0011

5. As shown, the agreement for the band positions is quite satisfactory with the largest deviation at ν_6, which has been discussed above. However, their intensities from different resources, as also shown in Table I, are quite different from each other, especially for ν_3. This suggests that the vibrational eigenvectors are significantly affected by the deuterated substitution, as given in Table II. As pointed in Ref.[27], the experimental absolute intensities obtained by different methodologies disagree by 50% or even more, particularly for strongly coupled levels, such as the ν_3 mode of CD$_2$OO, which is strongly coupled with other two modes: $\nu_6+\nu_7$, and $2\nu_8$. Therefore, the intensity borrowing effects will be pronounced. It is interesting to notice that for CH$_2$OO, the VCI-5 results on the same PES and DMS reproduced the experiment very well.

For CD$_2$OO, the calculated rotational constants are A''=2.0104 cm^{-1}, B''=0.3678 cm^{-1}, and C''=0.3099 cm^{-1} at its vibrational ground state (v=0). They are in excellent agreement with the experimental data: A''=2.0192 cm^{-1}, B''=0.3693 cm^{-1}

, and C''=0.3116 cm^{-1} [8]. The corresponding B3LYP/AVTZ results were A''=2.0737 cm^{-1}, B''=0.3647 cm^{-1}, and C''=0.3096 cm^{-1} [16]. The rotational constants, A', B', and C', of each specific vibrational state ($\nu_1-\nu_9$=1) are then calculated using the strategy described above, and included in Table II. The corresponding shifts of them from v=0 are also shown. For CH$_2$OO, the calculated shifts of the ν_7 and ν_8 modes were in excellent agreement with the observations [10]. Since no experiment measurement is available for comparison, the current results can be served as predictions. Table III lists the rotational parameters A'/A'', B'/B'', C'/C'' of CD$_2$OO calculated by VCI-5 and B3LYP [16], which are very helpful in simulating the rotational contours of each band.

IV. CONCLUSION

In this work, the ro-vibrational spectra of the CD$_2$OO species were theoretically investigated based on

full-dimensional accurate PES and DMS, which have demonstrated their excellent performance in simulating the experimental ro-vibrational spectra of CH_2OO with high resolution. In particular, the nine fundamental vibrational bands were determined by the VCI approach, which is efficient to provide reliable estimations for these states in this study. The agreement with the available experiment is satisfactory. However, the calculated infrared intensities deviate apparently from the experiment. It is interesting to note that our previous simulated vibrational frequencies and infrared intensities were in excellent agreement with experiment for CH_2OO on the same PES and DMS. For the rotational constants of the ground state, the VCI calculations agree quite well with the experiment. The rotational constants of the specific vibrational excited states are also determined and can be used for future spectroscopic simulations and experimental assignments. It is our hope that the current work can stimulate further experimental and theoretical investigations on this important molecule.

V. ACKNOWLEDGMENTS

[1] R. Criegee, Angew. Chem. Int. Ed. **14**, 745 (1975).
[2] D. Johnson and G. Marston, Chem. Soc. Rev. **37**, 699 (2008).
[3] O. Welz, J.D. Savee, D. L. Osborn, S. S. Vasu, C. J. Percival, D. E. Shallcross, and C. A. Taatjes, Science **335**, 204 (2012).
[4] C. A. Taatjes, D. E. Shallcross, and C. J. Percival, Phys. Chem. Chem. Phys. **16**, 1704 (2014).
[5] Y. P. Lee, J. Chem. Phys. **143**, 020901 (2015).
[6] D. L. Osborn and C. A. Taatjes, Int. Rev. Phys. Chem. **34**, 309 (2015).
[7] M. I. Lester and S. J. Klippenstein, Acc. Chem. Res. **51**, 978 (2018).
[8] M. Nakajima and Y. Endo, J. Chem. Phys. **139**, 101103 (2013).
[9] M. C. McCarthy, L. Cheng, K. N. Crabtree, O. Martinez, T. L. Nguyen, C. C. Womack, and J. F. Stanton, J. Phys. Chem. Lett. **4**, 4133 (2013).
[10] M. Nakajima, Q. Yue, J. Li, H. Guo, and Y. Endo, Chem. Phys. Lett. **621**, 129 (2015).
[11] Y. T. Su, Y. H. Huang, H. A. Witek, and Y. P. Lee, Science **340**, 174 (2013).
[12] Y. H. Huang, J. Li, H. Guo, and Y. P. Lee, J. Chem. Phys. **142**, 214301 (2015).
[13] Y. P. Chang, A. J. Merer, H. H. Chang, L. J. Jhang, W. Chao, and J. J. M. Lin, J. Chem. Phys. **146**, 244302 (2017).
[14] J. Li, S. Carter, J. M. Bowman, R. Dawes, D. Q. Xie, and H. Guo, J. Phys. Chem. Lett. **5**, 2364 (2014).
[15] H. G. Yu, S. Ndengue, J. Li, R. Dawes, and H. Guo, J. Chem. Phys. **143**, 084311 (2015).
[16] Y. H. Huang, Y. Nishimura, H. A. Witek, and Y. P. Lee, J. Chem. Phys. **145**, 044305 (2016).
[17] B. Jiang and H. Guo, J. Chem. Phys. **139**, 054112 (2013).
[18] J. Li, B. Jiang, and H. Guo, J. Chem. Phys. **139**, 204103 (2013).
[19] T. B. Adler, G. Knizia, and H. J. Werner, J. Chem. Phys. **127**, 221106 (2007).
[20] Y. Wang, X. Huang, B. C. Shepler, B. J. Braams, and J. M. Bowman, J. Chem. Phys. **134**, 094509 (2011).
[21] J. M. Bowman, S. Carter, and X. Huang, Int. Rev. Phys. Chem. **22**, 533 (2003).
[22] J. K. G. Watson, Mol. Phys. **15**, 479 (1968).
[23] J. M. Bowman, Acc. Chem. Res. **19**, 202 (1986).
[24] M. A. Ratner and R. B. Gerber, J. Phys. Chem. **90**, 20 (1986).
[25] S. Carter and J. M. Bowman, J. Chem. Phys. **108**, 4397 (1998).
[26] S. Carter, J. M. Bowman, and N. C. Handy, Theor. Chem. Acc. **100**, 191 (1998).
[27] R. Burcl, S. Carter, and N. C. Handy, Chem. Phys. Lett. **380**, 237 (2003).
[28] R. N. Zare, *Angular Momentum*, New York: John Wiley & Sons, Inc., (1988).